


Quantum routing of single photons within a specified frequency rangeXin Zhang and Xingmin Li ^{*}*School of Sciences, Hangzhou Dianzi University, Hangzhou 310018, China*

(Received 30 November 2023; accepted 22 April 2024; published 6 May 2024)

The quantum routing of single photons takes the central role in an optical quantum network. The matching between the routing probability and the selected frequency of single photons limits the robustness and universality of the quantum router. Here, we investigate how to implement the quantum routing of single photons within bandwidth frequencies by two cavities embedding atoms acting as quantum nodes. We show that the routing capabilities of the single photons and the range of the frequencies can be manipulated by properly designing the chiral coupling strengths and the channel boundaries. Also, we demonstrate that the incident single photons, within bandwidth frequencies, can be completely routed to the targeted output port. This is particularly important to construct optical quantum networks within bandwidth frequencies in the future.

DOI: [10.1103/PhysRevA.109.053707](https://doi.org/10.1103/PhysRevA.109.053707)**I. INTRODUCTION**

A quantum network is the physical basis of quantum information technology and possesses many functions [1–5], which cannot be implemented in the classical network. Thus the quantum network has been widely investigated and has been used to explore quantum sensing, quantum communication, quantum computing, etc. [6–11]. A quantum router is the basic element of the quantum network and it can distribute the quantum signals from one input port to multiple output ports [12–15].

Researching the quantum routing of single photons is quite important for the implementation of the optical quantum network. Until now, various systems have been used to research quantum routing of single photons, such as circuit quantum electrodynamics (QED) [16,17], optomechanical systems [18–20], cavity QED [21,22], giant atom(s) [23], and multilevel atom(s) [12,24]. In these systems, the single photons can be efficiently routed to the nonincident channels with specific frequency, but routing probabilities will rapidly diminish when the frequencies of the single photons are outside the designed region. Therefore, how to promote the quantum routing of single photons within bandwidth frequencies is quite important.

Photons are the best carriers of the quantum signals and the photons propagating along the waveguide will retain the coherence better. The chiral coupling between the photon and the quantum emitter can determine the propagation of the photon [25–30]. Therefore, the chiral photon-emitter interaction in a waveguide system can be used to implement the desired quantum routing of single photons in optical quantum networks [4,31–35].

In this paper, we propose an approach to implement efficient quantum routing of single photons within bandwidth frequencies. In the waveguide quantum system, the Rabi

splitting of the transmission spectrum will appear due to the coupling between the cavity and atom [36]. We set two cavities embedding two-level atoms as the quantum nodes in the proposed quantum routing system. Then we can broaden the frequency range, corresponding the single photons routed to the nonincident waveguide, by designing the chiral coupling strength and phase shift. Therefore, the quantum routing of single photons within bandwidth frequencies can be implemented. Furthermore, we implement more efficient quantum routing by using the terminated channel to control the propagation of the single photons along the incident waveguide. With these designs, the network to implement the efficient quantum routing of single photons within bandwidth frequencies is in principle possible.

The work is structured as follows. In Sec. II, we design the quantum routing scheme by two cavities embedding two-level atoms acting as the quantum nodes. We investigate how to implement the quantum routing of single photons within bandwidth frequencies and modulate the routing probability by the chiral coupling strength and the phase shift. In Sec. III, we further improve the routing capability by using a terminated waveguide as the incident channel. We demonstrate how to increase the routing efficiency of single photons within bandwidth frequencies by the parameters. Finally, we summarize our work and discuss the feasibility of the proposal in Sec. IV.

II. MODULATING QUANTUM ROUTING OF SINGLE PHOTONS WITHIN BANDWIDTH FREQUENCIES

A simplified quantum routing structure of the single photons within bandwidth frequencies is depicted in Fig. 1. The incident single photons come from the left of the waveguide a and are routed to different channels by the quantum nodes located at x_1 and x_2 . A quantum node consists of a cavity and a two-level atom and chirally couples to both waveguides. Usually, the dissipation caused by environment is inescapable and it will reduce the routing probability of the photons in

^{*}xingminli@hdu.edu.cn

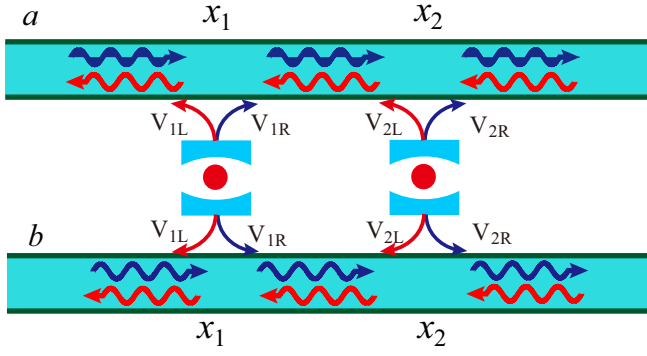


FIG. 1. Quantum routing of single photons within bandwidth frequencies. The quantum nodes, located at x_1 and x_2 , consist of cavities and two-level atoms, and chirally couple to the single photons propagating along the waveguides.

all directions. The influence caused by the cavity or atom is similar and the latter has been discussed in Ref. [14]. Here, we assume high quality cavities, then the influence will be trivial and can be neglected, and the atomic dipole-dipole interaction also is neglected for simplicity. Therefore, the Hamiltonian describing the chiral quantum routing system can be written as $H = H_s + H_p + H_{\text{int}}$ with [32,33]

$$\begin{aligned}
 H_s &= \sum_{j=1,2} \left[\left(\omega_{c_j} - i \frac{1}{\tau_j} \right) a_j^\dagger a_j + \left(\omega_{e_j} - \frac{i\Gamma_j}{2} \right) \sigma_j^+ \sigma_j^- \right. \\
 &\quad \left. + g_j (a_j \sigma_j^+ + a_j^\dagger \sigma_j^-) \right], \\
 H_p &= \sum_{n=a,b} i v_{gn} \int_{-\infty}^{\infty} dx \left[c_{nL}^\dagger(x) \left(\frac{\partial}{\partial x} \right) c_{nL}(x) \right. \\
 &\quad \left. - c_{nR}^\dagger(x) \left(\frac{\partial}{\partial x} \right) c_{nR}(x) \right], \\
 H_{\text{int}} &= \sum_{\substack{j=1,2 \\ n=a,b}} \int_{-\infty}^{\infty} dx \delta(x-x_j) [V_{jR} c_{nR}^\dagger(x) a_j \\
 &\quad + V_{jL} c_{nL}^\dagger(x) a_j + \text{H.c.}], \quad (1)
 \end{aligned}$$

where we set $\hbar = 1$. The first term H_s describes the cavities, the two-level atoms, and the interactions between the cavities and atoms. $j = 1, 2$ stands the j th cavity or atom. ω_{c_j} and ω_{e_j} are the resonance frequency of the cavity mode and the atomic transition frequency between the excited state $|e\rangle$ and the ground state $|g\rangle$. $a_j^\dagger(a_j)$ and $\sigma_j^+(\sigma_j^-)$ are the bosonic creation (annihilation) operator of the j th cavity mode and the raising (lowering) operator of the j th atom, respectively. g_j is the coupling strength between the cavity and the atom at x_j . $\frac{1}{\tau_j}$ and $\frac{\Gamma_j}{2}$ are the dissipation rates of the j th cavity and atom, respectively. The second term H_p describes the photon propagating along the waveguides with the order number $n = a, b$. v_{gn} is the group velocity of the photon propagating along the waveguide; $c_{nR(L)}^\dagger(x)$ [$c_{nR(L)}(x)$] is the bosonic creation (annihilation) operator of the photon propagating along the

waveguide n in the right(left) [$R(L)$] direction. The third term H_{int} describes the chiral interaction between the waveguides and the cavities. $V_{jR(L)}$ is the chiral coupling strength between the j th cavity and the photon propagating along the $R(L)$ direction.

The single-excitation eigenstate of the quantum routing system can be written as

$$\begin{aligned}
 |\Psi(x)\rangle &= \int_{-\infty}^{\infty} dx \sum_{n=a,b} [\phi_{nR}(x) c_{nR}^\dagger(x) + \phi_{nL}(x) c_{nL}^\dagger(x)] |\emptyset\rangle \\
 &\quad + \sum_{j=1,2} (e_{c_j} a_j^\dagger + e_{a_j} \sigma_j^+) |\emptyset\rangle, \quad (2)
 \end{aligned}$$

where $|\emptyset\rangle$ denotes the vacuum state. $\phi_{nR(L)}(x)$ stands for the probabilistic amplitude of the single photons propagating along waveguide n in the $R(L)$ direction and e_{c_j} and e_{a_j} denote the excitation amplitudes of the cavity j and the atom j , respectively. The probabilistic amplitudes of the single photons propagating along the $R(L)$ direction in the waveguides can be expressed as [22]

$$\begin{aligned}
 \phi_{aR}(x) &= e^{iqx} [\theta(x_1 - x) + t_{12} \theta(x - x_1) \theta(x_2 - x) \\
 &\quad + t \theta(x - x_2)], \\
 \phi_{aL}(x) &= e^{-iqx} [r \theta(x_1 - x) + r_{12} \theta(x - x_1) \theta(x_2 - x)], \\
 \phi_{bR}(x) &= e^{ikx} [t_R \theta(x - x_2) + t_{R12} \theta(x - x_1) \theta(x_2 - x)], \quad (3) \\
 \phi_{bL}(x) &= e^{-ikx} [t_L \theta(x_1 - x) + t_{L12} \theta(x - x_1) \theta(x_2 - x)].
 \end{aligned}$$

Here, t_{12} and t are the transmitted amplitudes of the photon in these areas: $x_1 < x < x_2$ and $x > x_2$ in the waveguide a , respectively. Correspondingly, r and r_{12} stand for the reflected amplitudes of the photon in these areas: $x < x_1$ and $x_1 < x < x_2$. Meanwhile, $t_R(t_L)$ is the transferred amplitudes in $x > x_2(x < x_1)$ along waveguide b and $t_{R12}(t_{L12})$ is the right (left) transferred amplitude in $x_1 < x < x_2$ along waveguide b . Also, q and k are the wave vectors in waveguides and satisfy $q \cdot v_{ga} = k \cdot v_{gb} = E$. Here, E is the eigenfrequency of the

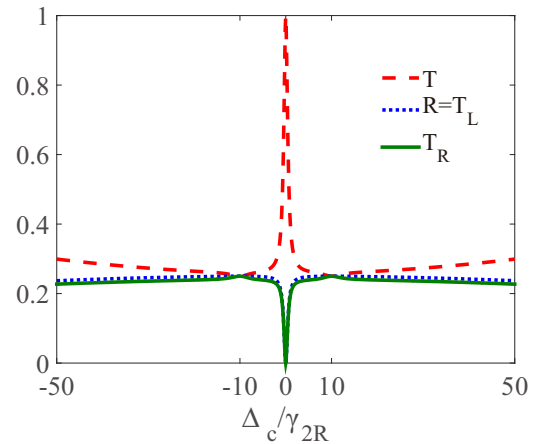


FIG. 2. Transmitted, reflected, and the routing probabilities T , R , T_L , and T_R versus the detuning Δ_c/γ_{2R} with the decay rates $\gamma_{1R}/\gamma_{2R} = \gamma_{1L}/\gamma_{2R} = 100$, $\gamma_{2L}/\gamma_{2R} = 10$, the coupling strength $g_1/\gamma_{2R} = g_2/\gamma_{2R} = 10$, and the phase shift $\theta = \pi$

single-excitation quantum routing system and is also equal to the frequency of the incident photons.

Here, we assume the cavity is high quality, then we can neglect the intrinsic dissipation of the cavity for simplicity

$$\begin{aligned}
 t &= \frac{-\left(i\Delta_{c1}\gamma_{1L} - g_1^2 + \Delta_{c1}\Delta_{e1}\right)\left(i\Delta_{c2}\gamma_{2L} - g_2^2 + \Delta_{c2}\Delta_{e2}\right) - \frac{2\Delta_{c1}\Delta_{c2}V_{1R}V_{2R}V_{1L}V_{2L}}{v_g^2} e^{2i\theta} + \Delta_{c1}\Delta_{c2}\gamma_{1R}\gamma_{2R}}{-\frac{4\Delta_{c1}\Delta_{c2}V_{1R}V_{2R}V_{1L}V_{2L}}{v_g^2} e^{2i\theta} - \left(i\Delta_{c1}\gamma_{1R} + i\Delta_{c1}\gamma_{1L} - g_1^2 + \Delta_{c1}\Delta_{e1}\right)\left(i\Delta_{c2}\gamma_{2R} + i\Delta_{c2}\gamma_{2L} - g_2^2 + \Delta_{c2}\Delta_{e2}\right)}, \\
 T_L = r &= \frac{\frac{i\Delta_{c1}V_{1R}V_{1L}}{v_g}\left(i\Delta_{c2}\gamma_{2R} + i\Delta_{c2}\gamma_{2L} - g_2^2 + \Delta_{c2}\Delta_{e2}\right) - \frac{i\Delta_{c2}V_{2R}V_{2L}}{v_g}\left(i\Delta_{c1}\gamma_{1R} + i\Delta_{c1}\gamma_{1L} + g_1^2 - \Delta_{c1}\Delta_{e1}\right)e^{2i\theta}}{-\frac{4\Delta_{c1}\Delta_{c2}V_{1R}V_{2R}V_{1L}V_{2L}}{v_g^2} e^{2i\theta} - \left(i\Delta_{c1}\gamma_{1R} + i\Delta_{c1}\gamma_{1L} - g_1^2 + \Delta_{c1}\Delta_{e1}\right)\left(i\Delta_{c2}\gamma_{2R} + i\Delta_{c2}\gamma_{2L} - g_2^2 + \Delta_{c2}\Delta_{e2}\right)}, \\
 T_R &= \frac{i\Delta_{c1}\gamma_{1R}\left(i\Delta_{c2}\gamma_{2L} - g_2^2 + \Delta_{c2}\Delta_{e2}\right) + i\Delta_{c2}\gamma_{2R}\left(i\Delta_{c1}\gamma_{1L} - g_1^2 + \Delta_{c1}\Delta_{e1}\right) + \frac{2\Delta_{c1}\Delta_{c2}V_{1R}V_{2R}V_{1L}V_{2L}}{v_g^2} e^{2i\theta}}{-\frac{4\Delta_{c1}\Delta_{c2}V_{1R}V_{2R}V_{1L}V_{2L}}{v_g^2} e^{2i\theta} - \left(i\Delta_{c1}\gamma_{1R} + i\Delta_{c1}\gamma_{1L} - g_1^2 + \Delta_{c1}\Delta_{e1}\right)\left(i\Delta_{c2}\gamma_{2R} + i\Delta_{c2}\gamma_{2L} - g_2^2 + \Delta_{c2}\Delta_{e2}\right)}, \quad (4)
 \end{aligned}$$

where $\Delta_{c1/c2} = E - \omega_{c1/c2}$ is the detuning between the photon and the cavity $1/2$ and $\Delta_{e1/e2} = E - \omega_{e1/e2}$ stands for the detuning between the photon and the atom $1/2$. $\gamma_{jL(R)} = V_{jL(R)}^2/v_g$ ($j = 1, 2$) is the decay rate of the single photons from the cavity j to the waveguides in the $L(R)$ direction. Above, $\theta = q(x_2 - x_1)$ is the phase shift of the routed single photons. Here, we consider $\Delta_{c1/c2} \ll E$, $\gamma_{jL(R)} \ll E$, $\frac{\theta}{2\pi} \ll \frac{E}{\gamma_{jL(R)}}$, and $\frac{\theta}{2\pi} \ll \frac{E}{\Delta_{c1/c2}}$; then we can neglect the fluctuation of the phase shift θ caused by the detunings. From Eq. (4), we can find that the transmitted, reflected, and transferred probabilities of the single photons satisfy the conservation equation $T + R + T_L + T_R = 1$, with $T = |t|^2$, $R = |r|^2$, $T_R = |t_R|^2$, and $T_L = |t_L|^2$.

In Fig. 2, we show how to implement quantum routing of single photons within bandwidth frequencies. Here, we set $\Delta_{e1} = \Delta_{e2} = \Delta_{c2} = \Delta_{c1} = \Delta_c$ for simplicity. Meanwhile, we assume the decay rates $\gamma_{1R}/\gamma_{2R} = \gamma_{1L}/\gamma_{2R} = 100$, $\gamma_{2L}/\gamma_{2R} = 10$, the coupling strengths $g_1/\gamma_{2R} = g_2/\gamma_{2R} = 10$, and the phase shift $\theta = \pi$. We can see that the routing probabilities T_L and T_R , the transmitted probability T , and the reflected probability R are all greater than 0.2 within bandwidth frequencies except for $\Delta_c/\gamma_{2R} \sim 0$. That means we can efficiently route the single photons to the nonincident waveguide within bandwidth frequency range. When the detuning $|\Delta_c/\gamma_{2R}| = 10$, the probabilities satisfy $T = R = T_L = T_R = 0.25$ and the routing probabilities T_L and T_R reach the maximum value. However, the single photons will mainly transmit the waveguide a with the detuning $\Delta_c/\gamma_{2R} \sim 0$. This result provides a robust approach to route the single photons within bandwidth frequencies.

In order to further investigate how to modulate the quantum routing process by the chiral coupling parameters, we first assume the coupling strengths $g_1/\gamma_{2R} = g_2/\gamma_{2R} = 10$, the decay rates $\gamma_{1R}/\gamma_{2R} = 100$ and $\gamma_{2L}/\gamma_{2R} = 10$, and the phase shift $\theta = \pi$. In Fig. 3, we show that the quantum routing probabilities T_L and T_R are modulated by the chiral decay rate γ_{1L}/γ_{2R} and the detuning Δ_c . From Fig. 3(a), the distribution of routing probability T_L is symmetrical on $\Delta_c = 0$ and T_L is 0 at $\Delta_c = 0$. The routing probability T_L can be stable within bandwidth frequencies and can reach the maximum value 0.25. For a fixed detuning Δ_c , the routing probability T_L increases with the chiral decay rate γ_{1L} until

[22]. Therefore, we can set $\frac{1}{\tau_1} = \frac{1}{\tau_2} = \frac{\Gamma_1}{2} = \frac{\Gamma_2}{2} = 0$ in the following discussion. Taking $x_1 = 0$, $k = q$, and $v_{ga} = v_{gb} = v_g$ for simplicity, we can get the amplitudes t , r , t_L , and t_R by solving the equation $H|\Psi(x)\rangle = E|\Psi(x)\rangle$:

$\gamma_{1L} = \gamma_{1R} = 100\gamma_{2R}$ and then decreases with γ_{1L} . Meanwhile, we can find that the routing probability T_L evolves fastest at $\Delta_c/\gamma_{2R} = \pm 10$. In Fig. 3(b), we can find that the distribution of routing probability T_R is also symmetrical on $\Delta_c = 0$, but the maximum routing probability in the R direction T_R can reach 100%. Meanwhile, the efficient routing probability T_R within bandwidth frequencies corresponds to the chiral decay rate $\gamma_{1L} < \gamma_{1R}$, the area of which is complementary with T_L .

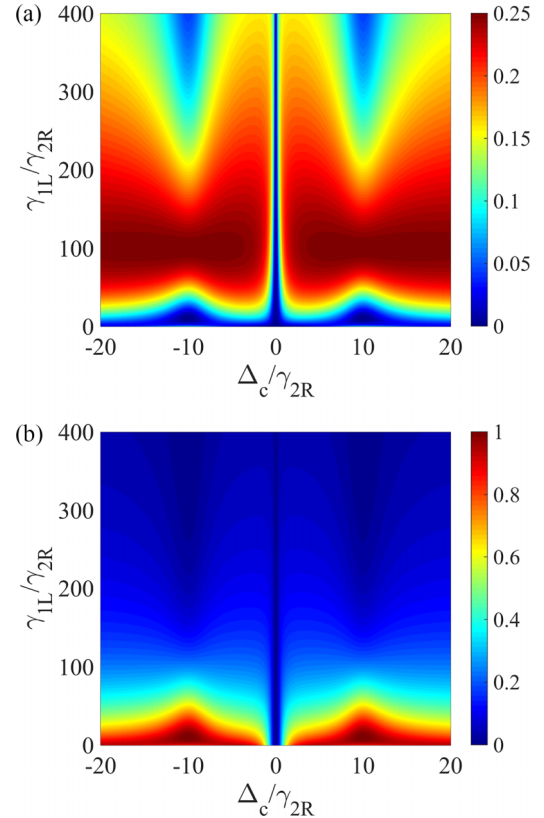


FIG. 3. (a) L direction routing probability T_L and (b) R direction routing probability T_R versus the detuning Δ_c/γ_{2R} and chiral decay rate γ_{1L}/γ_{2R} with $\gamma_{1R}/\gamma_{2R} = 100$, $\gamma_{2L}/\gamma_{2R} = 10$, $\theta = \pi$, and $g_1/\gamma_{2R} = g_2/\gamma_{2R} = 10$.

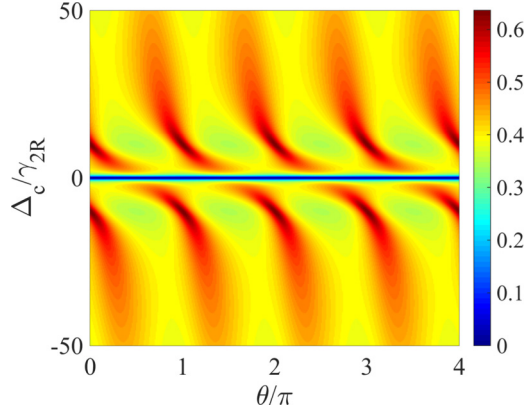


FIG. 4. Quantum routing probability T_R versus the phase shift θ and detuning Δ_c/γ_{2R} with coupling strength $g_1/\gamma_{2R} = g_2/\gamma_{2R} = 10$ and chiral decay rates $\gamma_{1L}/\gamma_{2R} = 50$, $\gamma_{1R}/\gamma_{2R} = 100$, and $\gamma_{2L}/\gamma_{2R} = 10$.

Here, T_R decreases monotonically with γ_{1L}/γ_{2R} . Therefore, we can also completely route the single photons within bandwidth frequencies to the nonincident waveguide by taking the chiral decay rate $\gamma_{1L} \ll \gamma_{1R}$. Here, the incident direction of the photon influences the asymmetry of the maximum probabilities of T_L and T_R . The routing probabilities can be changed from T_L to T_R with the incident direction of the photon and chiral decay rates being reversed.

The periodicity of the routing probability T_R is also investigated and shown in Fig. 4. Here, we assume the coupling strength $g_1/\gamma_{2R} = g_2/\gamma_{2R} = 10$ and chiral decay rates $\gamma_{1L}/\gamma_{2R} = 50$, $\gamma_{1R}/\gamma_{2R} = 100$, and $\gamma_{2L}/\gamma_{2R} = 10$. Then we can find that the period of T_R , depending on the phase shift, is π . And the maximum value of T_R is mainly at the phase shift $\theta = 0, \pi, 2\pi, \dots$

III. EFFICIENT QUANTUM ROUTING OF SINGLE PHOTONS WITHIN BANDWIDTH FREQUENCIES

In the above section, the quantum router can route the single photons to the nonincident waveguide within bandwidth frequencies, but the routing probability in the L direction (i.e., T_L) is quite low. In this section, we propose a high-efficiency quantum routing scheme, using a terminated waveguide as the incident channel, as shown in Fig. 5. The cavities couple to the both waveguides at x_1 and x_2 ($x_1 < x_2 < 0$) and the end of the terminated waveguide is assumed to be $x_3 = 0$. Then the Hamiltonian of this quantum routing system can be written as $H = H_{pt} + H_{int} + H_s + H_b$. Here, H_s is the same as Eq. (1).

H_{pt} describes the single photons propagating in both waveguides and can be represented as

$$H_{pt} = \int_{-\infty}^0 iv_g dx \left[c_{aL}^\dagger(x) \frac{\partial}{\partial x} c_{aL}(x) - c_{aR}^\dagger(x) \frac{\partial}{\partial x} c_{aR}(x) \right] + \int_{-\infty}^{\infty} iv_g dx \left[c_{bL}^\dagger(x) \frac{\partial}{\partial x} c_{bL}(x) - c_{bR}^\dagger(x) \frac{\partial}{\partial x} c_{bR}(x) \right]. \quad (5)$$

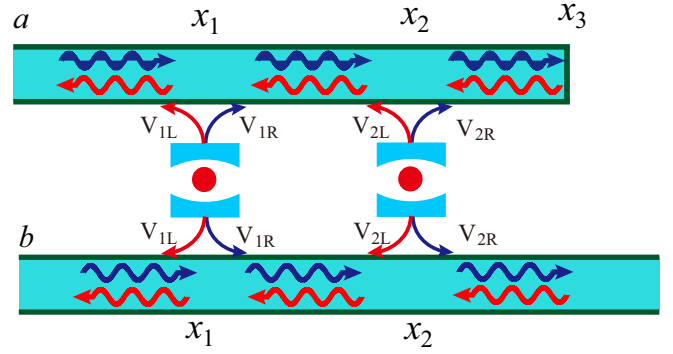


FIG. 5. Efficient quantum routing of single photons within bandwidth frequencies with a terminated waveguide being the incident channel. The quantum nodes, located at x_1 and x_2 , consist of a cavity and a two-level atom. The end of the terminated waveguide is $x_3 = 0$.

The interaction between the single photons and the cavities at x_1 and x_2 can be written as

$$H_{int} = \sum_{\substack{j=1,2 \\ m=R,L}} \int_{-\infty}^0 dx \delta(x-x_j) [V_{jm} c_{am}^\dagger(x) a_j + \text{H.c.}] + \sum_{\substack{j=1,2 \\ m=R,L}} \int_{-\infty}^{\infty} dx \delta(x-x_j) [V_{jm} c_{bm}^\dagger(x) a_j + \text{H.c.}], \quad (6)$$

with $m = R, L$ being the direction.

H_b describes the single photons' action of the boundary at $x_3 = 0$ in the terminated waveguide and is given by [22,37]

$$H_b = \int_{-\infty}^{0^+} dx \delta(x-x_3) [i2v_g c_{aL}^\dagger(x) c_{aR}(x) + \text{H.c.}]. \quad (7)$$

Then the single-excitation wave function of this quantum routing system can be expressed as

$$|\Psi(x)\rangle = \int_{-\infty}^0 dx [\phi_{aR}(x) c_{aR}^\dagger(x) + \phi_{aL}(x) c_{aL}^\dagger(x)] |\emptyset\rangle + \int_{-\infty}^{\infty} [\phi_{bR}(x) c_{bR}^\dagger(x) + \phi_{bL}(x) c_{bL}^\dagger(x)] |\emptyset\rangle + e_{c1} a_1^\dagger |\emptyset\rangle + e_{a1} \sigma_1^+ |\emptyset\rangle + e_{c2} a_2^\dagger |\emptyset\rangle + e_{a2} \sigma_2^+ |\emptyset\rangle. \quad (8)$$

The incident waveguide is terminated at x_3 ; then the probabilistic amplitudes of the single photons propagating along the $R(L)$ direction in the waveguides can be expressed as [22]

$$\begin{aligned} \phi_{aR}(x) &= e^{iqx} [\theta(x_1-x) + t_{a12}\theta(x-x_1)\theta(x_2-x) \\ &\quad + t_{a23}\theta(x-x_2)\theta(x_3-x)], \\ \phi_{aL}(x) &= e^{-iqx} [r_2\theta(x_1-x) + r_{a12}\theta(x-x_1)\theta(x_2-x) \\ &\quad + r_{a23}\theta(x-x_2)\theta(x_3-x)], \\ \phi_{bR}(x) &= e^{iqx} [t_{bR2}\theta(x-x_2) + t_{b12}\theta(x-x_1)\theta(x_2-x)], \\ \phi_{bL}(x) &= e^{-iqx} [t_{bL2}\theta(x_1-x) + r_{b12}\theta(x-x_1)\theta(x_2-x)]. \end{aligned} \quad (9)$$

Here, t_{a12} and t_{a23} are the transmitted amplitudes of the photon in these areas: (x_1, x_2) and (x_2, x_3) in waveguide

a , respectively. Correspondingly, r_2 , r_{a12} , and r_{a23} stand for the reflected amplitudes of the photon in these areas: $x < x_1$, (x_1, x_2) , and (x_2, x_3) in waveguide a . t_{bR2} (t_{bL2}) and

t_{b12} (r_{b12}) are the transferred amplitudes in $x > x_2$ ($x < x_1$) and $(x_1, x_2)[(x_1, x_2)]$ in the waveguide b .

Solving the equation $H|\Psi(x)\rangle = E|\Psi(x)\rangle$, we can get the amplitudes r_2 , t_{bR2} , and t_{bL2} :

$$\begin{aligned}
 A &= \frac{4\Delta_{c1}\Delta_{c2}V_{1R}V_{2R}V_{1L}V_{2L}}{v_g^2 e^{i2\theta_1}} e^{i2\theta_2} + \frac{\Delta_{c1}V_{1R}V_{1L}}{v_g e^{i2\theta_1}} (\Delta_{c2}\gamma_{2R} + \Delta_{c2}\gamma_{2L} - ig_2^2 + i\Delta_{c2}\Delta_{e2}) \\
 &\quad - (\Delta_{c1}\gamma_{1R} + \Delta_{c1}\gamma_{1L} + ig_1^2 - i\Delta_{c1}\Delta_{e1}) \left(\Delta_{c2}\gamma_{2R} + \Delta_{c2}\gamma_{2L} + ig_2^2 - i\Delta_{c2}\Delta_{e2} + \frac{\Delta_{c2}V_{2R}V_{2L}}{v_g e^{i2\theta_2}} \right), \\
 r_2 &= \frac{\frac{\Delta_{c1}V_{1R}V_{1L}}{v_g} e^{i2\theta_1} (\Delta_{c2}\gamma_{2R} + \Delta_{c2}\gamma_{2L} + \frac{\Delta_{c2}V_{2R}V_{2L}}{v_g} e^{-i2\theta_2} + ig_2^2 - i\Delta_{c2}\Delta_{e2}) - \Delta_{c1}\Delta_{c2}(\gamma_{1R}\gamma_{2R} + \gamma_{1L}\gamma_{2L})}{A} \\
 &\quad + \frac{\frac{\Delta_{c2}V_{2R}V_{2L}}{v_g} e^{i2\theta_2} (-\Delta_{c1}\gamma_{1R} - \Delta_{c1}\gamma_{1L} + \frac{\Delta_{c1}V_{1R}V_{1L}}{v_g} e^{-i2\theta_1} + ig_1^2 - i\Delta_{c1}\Delta_{e1}) - (-ig_1^2 + i\Delta_{c1}\Delta_{e1})(-ig_2^2 + i\Delta_{c2}\Delta_{e2})}{A}, \\
 t_{bR2} &= \frac{\frac{\Delta_{c1}V_{1R}V_{1L}}{v_g} e^{-i2\theta_1} (-\Delta_{c2}\gamma_{2L} - \Delta_{c2}\gamma_{2R} - \frac{2\Delta_{c2}V_{2R}V_{2L}}{v_g} e^{i2\theta_2} + ig_2^2 - i\Delta_{c2}\Delta_{e2}) + \Delta_{c1}\gamma_{1R}(\Delta_{c2}\gamma_{2L} + ig_2^2 - i\Delta_{c2}\Delta_{e2})}{A} \\
 &\quad + \frac{\frac{\Delta_{c2}V_{2R}V_{2L}}{v_g} e^{-i2\theta_2} (\Delta_{c1}\gamma_{1L} + \Delta_{c1}\gamma_{1R} + ig_1^2 - i\Delta_{c1}\Delta_{e1}) + \Delta_{c2}\gamma_{2R}(\Delta_{c1}\gamma_{1L} + ig_1^2 - i\Delta_{c1}\Delta_{e1})}{A}, \\
 t_{bL2} &= \frac{\frac{\Delta_{c1}V_{1R}V_{1L}}{v_g} e^{i2\theta_1} (\Delta_{c2}\gamma_{2L} + \Delta_{c2}\gamma_{2R} + \frac{\Delta_{c2}V_{2R}V_{2L}}{v_g} e^{-i2\theta_2} + ig_2^2 - i\Delta_{c2}\Delta_{e2}) + \Delta_{c1}\gamma_{1L}(ig_2^2 - i\Delta_{c2}\Delta_{e2})}{A} \\
 &\quad + \frac{\frac{\Delta_{c2}V_{2R}V_{2L}}{v_g} e^{i2\theta_2} (-\Delta_{c1}\gamma_{1L} - \Delta_{c1}\gamma_{1R} - \frac{\Delta_{c1}V_{1R}V_{1L}}{v_g} e^{-i2\theta_1} + ig_1^2 - i\Delta_{c1}\Delta_{e1}) + \Delta_{c2}\gamma_{2L}(ig_1^2 - i\Delta_{c1}\Delta_{e1})}{A}. \tag{10}
 \end{aligned}$$

Above, we set $\theta_1 = q(x_1 - x_3) < \theta_2 = q(x_2 - x_3) < 0$. The reflected and transferred probabilities satisfy the conservation equation $R_2 + T_{bR2} + T_{bL2} = 1$ with $R_2 = |r_2|^2$, $T_{bR2} = |t_{bR2}|^2$, and $T_{bL2} = |t_{bL2}|^2$.

How to modulate quantum routing probabilities T_{bR2} and T_{bL2} by the chiral coupling is shown in Figs. 6(a)–6(d). Here, we assume the detunings $\Delta_{e1} = \Delta_{e2} = \Delta_{c2} = \Delta_{c1} = \Delta_c$, the coupling strength $g_1/\gamma_{2R} = g_2/\gamma_{2R} = 10$, and the phases $\theta_1 = -\pi$, $\theta_2 = -\pi/2$. For the resonance incident single photons (i.e., $\Delta_c = 0$), the photons will be completely reflected (i.e., $R_2 = 100\%$). When the detuning increases to $|\Delta_c/\gamma_{2R}| = 10$ (i.e., $|\Delta_c| = g_1 = g_2$), the single photons will be completely routed to the waveguide b along the L direction (i.e., $T_{bL2} = 100\%$). In Fig. 6(a), we assume the chiral decay rates $\gamma_{1L}/\gamma_{2R} = 150$, $\gamma_{1R}/\gamma_{2R} = 100$, and $\gamma_{2L}/\gamma_{2R} = 1$ (i.e., $\gamma_{1L} > \gamma_{1R}$ and $\gamma_{2L} = \gamma_{2R}$) and we can find that the quantum routing is much more efficient than the previous scheme and the quantum routing probabilities satisfy $T_{bL2} > T_{bR2}$ with $|\Delta_c/\gamma_{2R}| > 10$. In Fig. 6(b), the quantum routing probabilities become $T_{bL2} = T_{bR2}$ with the chiral decay rates $\gamma_{1L}/\gamma_{2R} = \gamma_{1R}/\gamma_{2R} = 100$ and $\gamma_{2L}/\gamma_{2R} = 1$ (i.e., $\gamma_{1L} = \gamma_{1R}$ and $\gamma_{2L} = \gamma_{2R}$). When the chiral decay rates become $\gamma_{1L}/\gamma_{2R} = 50$, $\gamma_{1R}/\gamma_{2R} = 100$, and $\gamma_{2L}/\gamma_{2R} = 1$ (i.e., $\gamma_{1L} < \gamma_{1R}$ and $\gamma_{2L} = \gamma_{2R}$), the quantum routing probabilities become $T_{bL2} < T_{bR2}$ as shown in Fig. 6(c). In Fig. 6(d), the chiral decay rates become $\gamma_{1L}/\gamma_{2R} = 100$, $\gamma_{1R}/\gamma_{2R} = 100$, and $\gamma_{2L}/\gamma_{2R} = 10$ (i.e., $\gamma_{1L} = \gamma_{1R}$ and $\gamma_{2L} > \gamma_{2R}$) and the routing probability in the L direction is greater than the probability in the R direction (i.e., $T_{bL2} > T_{bR2}$). These results show that this quantum routing scheme can much more efficiently route the single photons to

the nonincident waveguide within bandwidth frequencies, the chiral decay rates γ_{1L} and γ_{1R} can determine the distribution of the quantum routing probabilities in the L and R directions

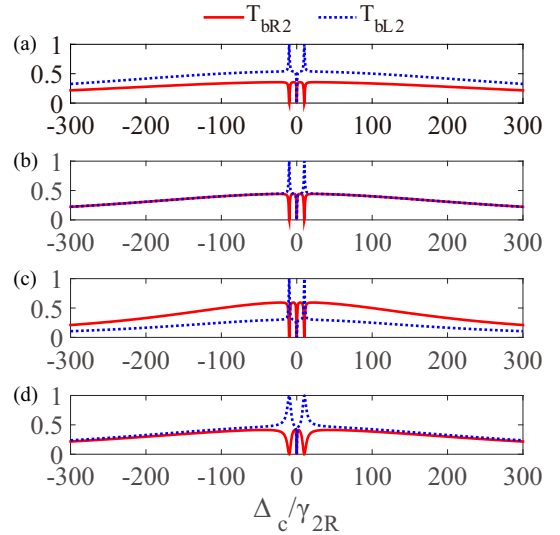


FIG. 6. Quantum routing probabilities T_{bR2} and T_{bL2} versus the detuning Δ_c/γ_{2R} for the selected detunings $\Delta_{e1} = \Delta_{e2} = \Delta_{c2} = \Delta_{c1} = \Delta_c$, the coupling strength $g_1/\gamma_{2R} = g_2/\gamma_{2R} = 10$, and the phases $\theta_1 = -\pi$, $\theta_2 = -\pi/2$. (a) The chiral decay rates $\gamma_{1L}/\gamma_{2R} = 150$, $\gamma_{1R}/\gamma_{2R} = 100$, and $\gamma_{2L}/\gamma_{2R} = 1$; (b) the chiral decay rates $\gamma_{1L}/\gamma_{2R} = \gamma_{1R}/\gamma_{2R} = 100$ and $\gamma_{2L}/\gamma_{2R} = 1$; (c) the chiral decay rates $\gamma_{1L}/\gamma_{2R} = 50$, $\gamma_{1R}/\gamma_{2R} = 100$, and $\gamma_{2L}/\gamma_{2R} = 1$; (d) the chiral decay rates $\gamma_{1L}/\gamma_{2R} = \gamma_{1R}/\gamma_{2R} = 100$ and $\gamma_{2L}/\gamma_{2R} = 10$.

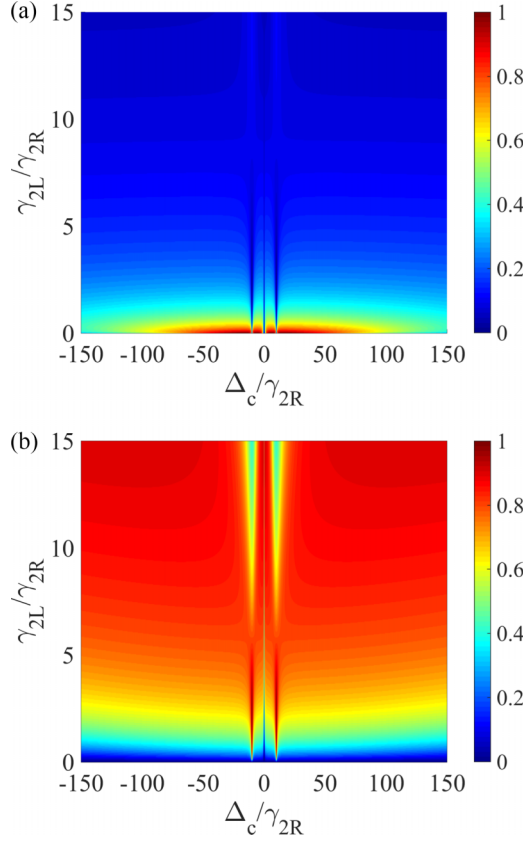


FIG. 7. Quantum routing probabilities (a) T_{br2} and (b) T_{bl2} versus the detuning Δ_c/γ_{2R} and the chiral decay rate γ_{2L}/γ_{2R} with the decay rates $\gamma_{1L}/\gamma_{2L} = \gamma_{1R}/\gamma_{2R} = 100$, coupling strengths $g_1/\gamma_{2R} = g_2/\gamma_{2R} = 10$, and the phases $\theta_1 = -\pi$, $\theta_2 = -\pi/2$.

(i.e., $T_{bl2}/T_{br2} \propto \gamma_{1L}/\gamma_{1R}$), and the chiral decay rates γ_{2L} and γ_{2R} have a similar effect. In order to further investigate the quantum routing scheme with the terminated waveguide, we assume the decay rates $\gamma_{1L}/\gamma_{2L} = \gamma_{1R}/\gamma_{2R} = 100$, coupling strengths $g_1/\gamma_{2R} = g_2/\gamma_{2R} = 10$, and the phases $\theta_1 = -\pi$, $\theta_2 = -\pi/2$. In Fig. 7(a), we show how to modulate the quantum routing probability T_{br2} by the chiral decay rate γ_{2L} and the detuning Δ_c . We find that the routing probability $T_{br2} \rightarrow 100\%$ with the chiral decay rate $\gamma_{2L}/\gamma_{2R} < 1$ and the bandwidth frequency being $|\Delta_c/\gamma_{2R}| < 50$. Here, the efficient quantum routing with bandwidth frequencies in the R direction mainly corresponds to the low chiral decay rate (e.g., $\gamma_{2L}/\gamma_{2R} < 1$). The routing probability T_{br2} increases as the chiral decay rate γ_{2L}/γ_{2R} corresponding to the detuning $\Delta_c/\gamma_{2R} = 0, \pm 10$, but decreases as the chiral decay rate γ_{2L}/γ_{2R} corresponding to the other detuning. The routing probability T_{bl2} versus the chiral decay rate γ_{2L}/γ_{2R} and the detuning Δ_c/γ_{2R} is shown in Fig. 7(b). Here, we find that the routing probability T_{bl2} decreases as γ_{2L}/γ_{2R} corresponding to the detuning $\Delta_c/\gamma_{2R} = 0, \pm 10$, but increases as the chiral decay rate γ_{2L}/γ_{2R} corresponding to the other detuning, even reaching 100% with chiral decay rate $\gamma_{2L}/\gamma_{2R} \simeq 15$. In Fig. 7(b), the efficient quantum routing with bandwidth frequencies in the L direction mainly corresponds to the large chiral decay rate (e.g., $\gamma_{2L}/\gamma_{2R} > 1$). Therefore, we can robustly modulate the single photons being routed to targeted

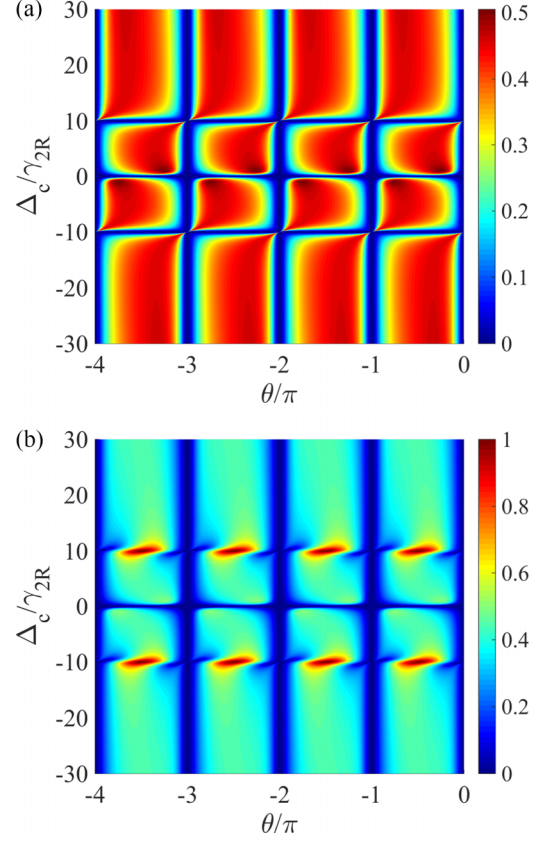


FIG. 8. Quantum routing probabilities (a) T_{br2} and (b) T_{bl2} versus the phase θ and the detuning Δ_c/γ_{2R} , for the decay rates $\gamma_{1R}/\gamma_{2R} = \gamma_{1L}/\gamma_{2R} = 100$, $\gamma_{2L} = \gamma_{2R}$ and the coupling strength $g_1/\gamma_{2R} = g_2/\gamma_{2R} = 10$.

output ports with targeted probability by the chiral decay rate γ_{2L} and detuning Δ_c . The phase shift between both cavities can also influence the distribution of the routing probabilities in the $R(L)$ direction. Here, we consider the phase shifts $\theta_2 = -\pi/2$ and $\theta_1 = \theta - \pi/2$, with θ being the phase shift between both cavities, and assume the decay rates $\gamma_{1R}/\gamma_{2R} = \gamma_{1L}/\gamma_{2R} = 100$, $\gamma_{2L} = \gamma_{2R}$ and the coupling strength $g_1/\gamma_{2R} = g_2/\gamma_{2R} = 10$. Then we show the quantum routing probabilities T_{br2} and T_{bl2} versus the phase θ and the detuning Δ_c/γ_{2R} in Figs. 8(a) and 8(b), respectively. In Fig. 8(a), we can find that the period of T_{br2} is π and the maximum value of T_{br2} can reach 50%. T_{br2} will decrease to 0 when the detuning satisfies $\Delta_c/\gamma_{2R} = 0, \pm 10$ or the phase shift becomes $\theta = -k\pi$ ($k = 0, 1, 2, 3, \dots$). In Fig. 8(b), we show that the period of T_{bl2} also is π and the maximum value of T_{bl2} can reach 100%. T_{bl2} will decrease to 0 with $\Delta_c/\gamma_{2R} = 0$ and $\theta = -k\pi$ and then it can reach 100% with $\Delta_c/\gamma_{2R} = \pm 10$ and $\theta = -\pi/2 - k\pi$. These results show that the efficient quantum routing of single photons within bandwidth frequency also can be implemented and the phase shift θ can modulate the matching of the routing probability and the detuning.

IV. SUMMARY AND CONCLUSIONS

In conclusion, we investigate how to modulate the quantum routing of single photons within bandwidth frequencies by

chiral cavity-photon coupling and cavity-atom interaction. We have shown that the routing probabilities in L and R directions are all greater than 20% within bandwidth frequencies in the normal four-port quantum router and the maximum probabilities are 25% and 100%, respectively. Using a terminated waveguide as the incident channel, we can implement more efficient quantum routing of single photons within bandwidth frequencies and the limit of the probabilities in L and R directions can all reach 100% within bandwidth frequencies. We also show that the chiral decay rates γ_{1L} , γ_{1R} , and γ_{2L} can determine the distribution of the routing probabilities in both directions. The phase period of the routing probabilities is π and the phase shift can also influence the quantum routing. It has been demonstrated that the coupling strength between the atom and light in the clockwise (cw) mode g_{cw} is much weaker than that between the atom and light in the counterclockwise (ccw) mode g_{ccw} (e.g., $\Gamma_{ccw} = g_{ccw}^2/\beta \approx 2\pi \times 48$ MHz and $\Gamma_{cw} = g_{cw}^2/\beta \approx 2\pi \times 1.7$ MHz with $\beta = 2\pi \times 3$ MHz) in experiment [38].

Considering the atom in the Zeeman state, the single photons propagating along the right (left) direction correspond to the cw (ccw) mode [38,39]. However, the roles of cw and ccw modes can be exchanged by preparing the atom in the opposite Zeeman ground state [38]. That means it can experimentally modulate the ratio Γ_{ccw}/Γ_{cw} from 0.035 to 28.23 by the external bias fields. These results demonstrate the feasibility of our quantum routing scheme.

We hope that our proposal can provide a feasible and robust approach to constructing the quantum networks within bandwidth frequencies.

ACKNOWLEDGMENTS

This research was supported by Zhejiang Provincial Natural Science Foundation of China under Grant No. LQ20A040006.

-
- [1] H. J. Kimble, The quantum internet, *Nature (London)* **453**, 1023 (2008).
- [2] S. Ritter, C. Nölleke, C. Hahn, A. Reiserer, A. Neuzner, M. Uphoff, M. Mücke, E. Figueroa, J. Bochmann, and G. Rempe, An elementary quantum network of single atoms in optical cavities, *Nature (London)* **484**, 195 (2012).
- [3] A. Reiserer and G. Rempe, Cavity-based quantum networks with single atoms and optical photons, *Rev. Mod. Phys.* **87**, 1379 (2015).
- [4] S. Mahmoodian, P. Lodahl, and A. S. Sørensen, Quantum networks with Chiral-Light-Matter interaction in waveguides, *Phys. Rev. Lett.* **117**, 240501 (2016).
- [5] P. C. Humphreys, N. Kalb, J. P. J. Morits, R. N. Schouten, R. F. L. Vermeulen, D. J. Twitchen, M. Markham, and R. Hanson, Deterministic delivery of remote entanglement on a quantum network, *Nature (London)* **558**, 268 (2018).
- [6] C. Monroe, Quantum information processing with atoms and photons, *Nature (London)* **416**, 238 (2002).
- [7] N. Gisin and R. Thew, Quantum communication, *Nat. Photon.* **1**, 165 (2007).
- [8] Y.-A. Chen, Q. Zhang, T.-Y. Chen *et al.*, An integrated space-to-ground quantum communication network over 4,600 kilometres, *Nature (London)* **589**, 214 (2021).
- [9] V. Giovannetti, S. Lloyd, and L. Maccone, Advances in quantum metrology, *Nat. Photon.* **5**, 222 (2011).
- [10] N. H. Nickerson, J. F. Fitzsimons, and S. C. Benjamin, Freely scalable quantum technologies using cells of 5-to-50 qubits with very lossy and noisy photonic links, *Phys. Rev. X* **4**, 041041 (2014).
- [11] T. Satoh, F. Le. Gall, and H. Imai, Quantum network coding for quantum repeaters, *Phys. Rev. A* **86**, 032331 (2012).
- [12] L. Zhou, L.-P. Yang, Y. Li, and C. P. Sun, Quantum routing of single photons with a cyclic three-level system, *Phys. Rev. Lett.* **111**, 103604 (2013).
- [13] K. Xia and J. Twamley, All-optical switching and router via the direct quantum control of coupling between cavity modes, *Phys. Rev. X* **3**, 031013 (2013).
- [14] X. Li and L. F. Wei, Designable single-photon quantum routings with atomic mirrors, *Phys. Rev. A* **92**, 063836 (2015).
- [15] S. Gyger, J. Zichi, L. Schweickert *et al.*, Efficient single-photon routing in a double-waveguide system with a mirror, *Nat. Commun.* **12**, 1408 (2021).
- [16] Y. T. Zhu and W. Z. Jia, Single-photon quantum router in the microwave regime utilizing double superconducting resonators with tunable coupling, *Phys. Rev. A* **99**, 063815 (2019).
- [17] K. S. Christensen, S. E. Rasmussen, D. Petrosyan, and N. T. Zinner, Coherent router for quantum networks with superconducting qubits, *Phys. Rev. Res.* **2**, 013004 (2020).
- [18] G. S. Agarwal and S. Huang, Optomechanical systems as single-photon routers, *Phys. Rev. A* **85**, 021801(R) (2012).
- [19] K. Fang, M. H. Matheny, X. Luan, and O. Painter, Optical transduction and routing of microwave phonons in cavity-optomechanical circuits, *Nat. Photon.* **10**, 489 (2016).
- [20] G. Li, X. Xiao, Y. Li, and X. Wang, Tunable optical nonreciprocity and a phonon-photon router in an optomechanical system with coupled mechanical and optical modes, *Phys. Rev. A* **97**, 023801 (2018).
- [21] M. Brekenfeld, D. Niemietz, J. D. Christesen *et al.*, A quantum network node with crossed optical fibre cavities, *Nat. Phys.* **16**, 647 (2020).
- [22] X. Li, J. Xin, G. Li, X.-M. Lu, and L. F. Wei, Quantum routings for single photons with different frequencies, *Opt. Express* **29**, 8861 (2021).
- [23] C. Wang, X.-S. Ma, and M.-T. Cheng, Giant atom-mediated single photon routing between two waveguides, *Opt. Express* **29**, 40116 (2021).
- [24] I. Shomroni, S. Rosenblum, Y. Lovsky, O. Bechler, G. Guendelman, and B. Dayan, All-optical routing of single photons by a one-atom switch controlled by a single photon, *Science* **345**, 903 (2014).
- [25] C.-H. Yan, L.-F. Wei, W.-Z. Jia, and J.-T. Shen, Controlling resonant photonic transport along optical waveguides by two-level atoms, *Phys. Rev. A* **84**, 045801 (2011).

- [26] I. Söllner, S. Mahmoodian, S. L. Hansen, L. Midolo, A. Javadi, T. Kiršanskė, G. Pregolato, H. El-Ella, E. H. Lee, J. D. Song, S. Stobbe, and P. Lodahl, Deterministic photon-emitter coupling in chiral photonic circuits, *Nat. Nanotechnol.* **10**, 775 (2015).
- [27] A. B. Young, A. C. T. Thijssen, D. M. Beggs, P. Androvitsaneas, L. Kuipers, J. G. Rarity, S. Hughes, and R. Oulton, Polarization engineering in photonic crystal waveguides for spin-photon entanglers, *Phys. Rev. Lett.* **115**, 153901 (2015).
- [28] B. le Feber, N. Rotenberg, and L. Kuipers, Nanophotonic control of circular dipole emission *Nat. Commun.* **6**, 6695 (2015).
- [29] R. J. Coles, D. M. Price, J. E. Dixon, B. Royall, E. Clarke, P. Kok, M. S. Skolnick, A. M. Fox, and M. N. Makhonin, Chirality of nanophotonic waveguide with embedded quantum emitter for unidirectional spin transfer, *Nat. Commun.* **7**, 11183 (2016).
- [30] P. Lodahl, S. Mahmoodian, S. Stobbe, A. Rauschenbeutel, P. Schneeweiss, J. Volz, H. Pichler, and P. Zoller, Chiral quantum optics, *Nature (London)* **541**, 473 (2017).
- [31] H. Pichler, T. Ramos, A. J. Daley, and P. Zoller, Quantum optics of chiral spin networks, *Phys. Rev. A* **91**, 042116 (2015).
- [32] C. Gonzalez-Ballester, E. Moreno, F. J. Garcia-Vidal, A. Gonzalez-Tudela, Nonreciprocal few-photon routing schemes based on chiral waveguide-emitter couplings, *Phys. Rev. A* **94**, 063817 (2016).
- [33] C.-H. Yan, Y. Li, H. Yuan, and L.-F. Wei, Targeted photonic routers with chiral photon-atom interactions, *Phys. Rev. A* **97**, 023821 (2018).
- [34] B. Poudyal and I. M. Mirza, Collective photon routing improvement in a dissipative quantum emitter chain strongly coupled to a chiral waveguide QED ladder, *Phys. Rev. Res.* **2**, 043048 (2020).
- [35] Y.-L. Ren, S.-L. Ma, J.-K. Xie, X.-K. Li, M.-T. Cao, and F.-L. Li, Nonreciprocal single-photon quantum router, *Phys. Rev. A* **105**, 013711 (2022).
- [36] J.-T. Shen and S. Fan, Theory of single-photon transport in a single-mode waveguide. I. Coupling to a cavity containing a two-level atom, *Phys. Rev. A* **79**, 023837 (2009).
- [37] M. Bradford and J.-T. Shen, Spontaneous emission in cavity QED with a terminated waveguide, *Phys. Rev. A* **87**, 063830 (2013).
- [38] M. Scheucher, A. Hilico, E. Will, J. Volz, and A. Rauschenbeutel, Quantum optical circulator controlled by a single chirally coupled atom, *Science* **354**, 1577 (2016).
- [39] C. Sayrin, C. Junge, R. Mitsch, B. Albrecht, D. O'Shea, P. Schneeweiss, J. Volz, and A. Rauschenbeutel, Nanophotonic optical isolator controlled by the internal state of cold atoms, *Phys. Rev. X* **5**, 041036 (2015).